Polymorphism in the negative thermal expansion material magnesium hafnium tungstate

Amy M. Gindhart and Cora Lind[a)]
Department of Chemistry, The University of Toledo, Toledo, Ohio 43606

Mark Green
National Institute of Standards and Technology, Gaithersburg, Maryland 20899-6102; and Department of Materials Science and Engineering, University of Maryland, College Park, Maryland 20742-2115

(Received 3 August 2007; accepted 25 September 2007)

Magnesium hafnium tungstate [$MgHf(WO_4)_3$] was synthesized by high-energy ball milling followed by calcination. The material was characterized by variable-temperature neutron and x-ray diffraction. It crystallized in space group $P2_1/a$ below 400 K and transformed to an orthorhombic structure at higher temperatures. The orthorhombic polymorph adopted space group *Pnma*, instead of the *Pnca* structure commonly observed for other $A_2(MO_4)_3$ materials (A = trivalent metal, M = Mo, W). In contrast, the monoclinic polymorphs appeared to be isostructural. Negative thermal expansion was observed in the orthorhombic phase with $\alpha_a = -5.2 \times 10^{-6}$ K^{-1}, $\alpha_b = 4.4 \times 10^{-6}$ K^{-1}, $\alpha_c = -2.9 \times 10^{-6}$ K^{-1}, $\alpha_V = -3.7 \times 10^{-6}$ K^{-1}, and $\alpha_l = -1.2 \times 10^{-6}$ K^{-1}. The monoclinic to orthorhombic phase transition was accompanied by a smooth change in unit-cell volume, indicative of a second-order phase transition.

I. INTRODUCTION

There has been significant interest in negative thermal expansion (NTE) materials.[1–8] Since NTE materials will contract upon heating rather than expand, their incorporation into composites could reduce the overall thermal expansion of the composite. Previous work in the $A_2(MO_4)_3$ system (A = trivalent metal, M = Mo, W) has shown that this thermal expansion behavior is highly dependent on the identity of the A^{3+} cation.[8–11] For trivalent ions up to the size of the smaller rare earths, the A cation is usually six coordinated, and the materials form either monoclinic or orthorhombic structures, the latter being the phase that exhibits NTE. For many compositions, a transition from monoclinic to orthorhombic symmetry is observed upon heating.

It has been shown that the A site in $A_2(WO_4)_3$ compounds can be substituted by a mixture of Hf^{4+} and Mg^{2+}.[12] $MgHf(WO_4)_3$ was reported to adopt an orthorhombic structure with space group *Pnma* at room temperature and 700 °C. Negative thermal expansion along the *a* and *c* axes, combined with positive expansion along *b*, were observed for $MgHf(WO_4)_3$, and it was argued that the mechanism of NTE should be the same as for "isostructural" $Sc_2(WO_4)_3$. However, all previous reports on NTE materials in the $A_2(MO_4)_3$ family assigned them to space group *Pnca*. *Pnma* and *Pnca* do not share a sub/supergroup relationship; in fact, the only common subgroups of *Pnma* and *Pnca* are $Pna2_1$ and $P2_1/c$.

In this paper, we report a detailed structural investigation on $MgHf(WO_4)_3$ by powder x-ray and neutron diffraction. The material was found to adopt a monoclinic structure below 400 K, and to transform to an orthorhombic polymorph that is not isostructural to $Sc_2(WO_4)_3$ at higher temperatures.

II. EXPERIMENTAL

$MgHf(WO_4)_3$ was prepared by ball milling and subsequent calcination. Magnesium carbonate, hafnium oxide, and tungsten oxide were milled for a total of 2 to 3 h in a molar ratio of 1:1:3. The powder was pressed into pellets and calcined at various temperatures ranging from 1173 to 1473 K in air.

The composition and structure of the powder samples were evaluated by x-ray diffraction (XRD) using a PANalytical (Westborough, MA) X-Pert Pro diffractometer with an X'celerator detector. Variable-temperature studies were carried out on a Scintag XDS-2000 diffractometer with a Moxtek (Orem, UT) detector and an Anton–Paar (Ashland, VA) variable-temperature stage with a platinum heater strip. Both instruments use Cu K_α radiation and Bragg–Brentano geometry. Data were

[a)]Address all correspondence to this author.
e-mail: cora.lind@utoledo.edu
DOI: 10.1557/JMR.2008.0013

collected from room temperature to 973 K using silicon as an internal standard.

Neutron powder diffraction data were collected at the BT-1 32 detector neutron powder diffractometer at the NCNR, NIST. A Cu(311) monochromator with a 90° take-off angle, $\lambda = 1.5403(2)$ Å, and in-pile collimation of 15 min of arc were used. Data were collected over the range of 3 to 168° 2θ with a step size of 0.05°. The sample was loaded in a vanadium sample container of 50 mm length and 6 mm diameter. Data were collected from 4 to 700 K. The diffraction data were analyzed by the Rietveld and Le Bail methods using FullProf.[13]

III. RESULTS AND DISCUSSION

Single-phase $MgHf(WO_4)_3$ was obtained by heating the ball-milled powder to 1373 K for 24 h. Temperatures below 1298 K only yielded impurity phases (HfO_2, WO_3, and $MgWO_4$). Phase pure $MgHf(WO_4)_3$ could be obtained between 1323 and 1423 K, while the pellets melted at 1433 K and higher temperatures. Ball milling appeared to be crucial for the preparation of the quarternary phase. Only binary and ternary oxides could be observed at all temperatures when heating pellets of material that had not been milled.

A slow, room-temperature XRD scan was collected for Rietveld analysis. Attempts to fit the data in an orthorhombic unit cell were unsuccessful. Several weak reflections were unaccounted for, even using the Le Bail method and with the symmetry lowered to *P*222. As many $A_2(MO_4)_3$ compounds adopt a monoclinic structure at low temperatures, the model for monoclinic $Al_2(MoO_4)_3$ (space group $P2_1/a$) was tested. An excellent fit could be obtained using this structure and mixed-cation occupancy Mg/Hf for all Al sites.

The thermal expansion and phase transition behavior of $MgHf(WO_4)_3$ was investigated using variable-temperature x-ray and neutron diffraction. Lattice constants from x-ray data were obtained by fixing the lattice parameter of the internal reference material to known values[14] and refining the lattice constants of $MgHf(WO_4)_3$ along with the sample height. For the neutron data, a zero-point error was refined along with the lattice constants. All data sets converged with zero-point errors of −0.071(1)°.

An absorption correction was applied to the neutron data, and all data were refined in $P2_1/a$ using the monoclinic structure of $Al_2(MoO_4)_3$ as a starting model. This model gave an excellent fit for the data up to 400 K (Fig. 1), but resulted in less than satisfactory agreement for the 550 and 700 K data sets. A full structural refinement of the 4 K data with mixed Mg/Hf cation occupancy on all four sites showed a strong preference for magnesium on two of the sites, and a strong preference for hafnium on the other two sites. As the refined occupancies suggested

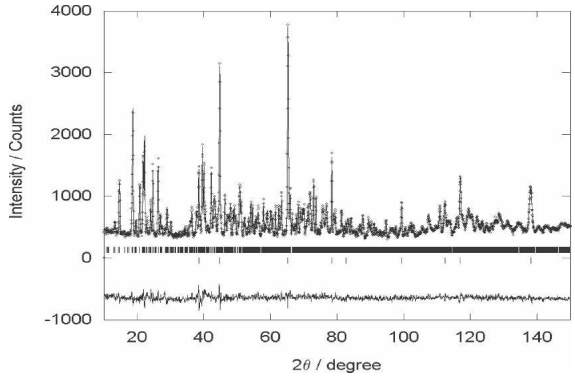

FIG. 1. Rietveld refinement of the neutron diffraction data of $MgHf(WO_4)_3$ collected at 4 K. Diamonds represent data points, the calculated pattern corresponds to the solid line, and a difference plot is shown below the pattern. Tick marks indicate peak positions for $MgHf(WO_4)_3$ (top) and Al from the heat shield (bottom).

complete cation ordering, the structure was refined with two pure Mg and two pure Hf sites. The final structural model is available as supplementary material.

For the XRD data, the monoclinic cell could account for the data up to 373 K. Some subtle changes were observed in the diffraction patterns above 400 K. This suggested a change in lattice symmetry, similar to what is observed for other $A_2(MO_4)_3$ compounds upon heating. However, the data could not be fitted with the orthorhombic $Al(MoO_4)_3$ structure in space group *Pnca*. This space group gave a less than satisfactory fit, both using a structural model and with the Le Bail method [Fig. 2(a)]. Indexing using Crysfire[15] returned an orthorhombic cell with high figures of merit for ITO,[16] DICVOL,[17] TREOR,[18] TAUP,[19] and KOHL.[20] Systematic absences pointed to *Pnma* as the highest possible symmetry. This difference in unit-cell symmetry could be related to the presence of two different cations on the octahedrally coordinated sites, and the tendency toward cation ordering observed during neutron data refinement of the monoclinic phase. Le Bail fits of each variable-temperature data set were carried out using this space group. The fits were excellent for the 473 K and above data sets [Fig. 2(b)], which were clearly orthorhombic, while the room-temperature data resulted in poor agreement between calculated and observed intensities. The orthorhombic unit cell in space group *Pnma* also gave good fits for the 550 and 700 K neutron diffraction data. Data collected above 873 K were not refined, as sample decomposition was observed. The lattice constants and unit-cell volumes were extracted from the refined data and are shown in Table I.

Very little change in cell volume was observed in the monoclinic region, followed by negative thermal expansion in the orthorhombic phase (Fig. 3). The expansion behavior in the orthorhombic phase is anisotropic, with positive thermal expansion along *b*, and negative thermal

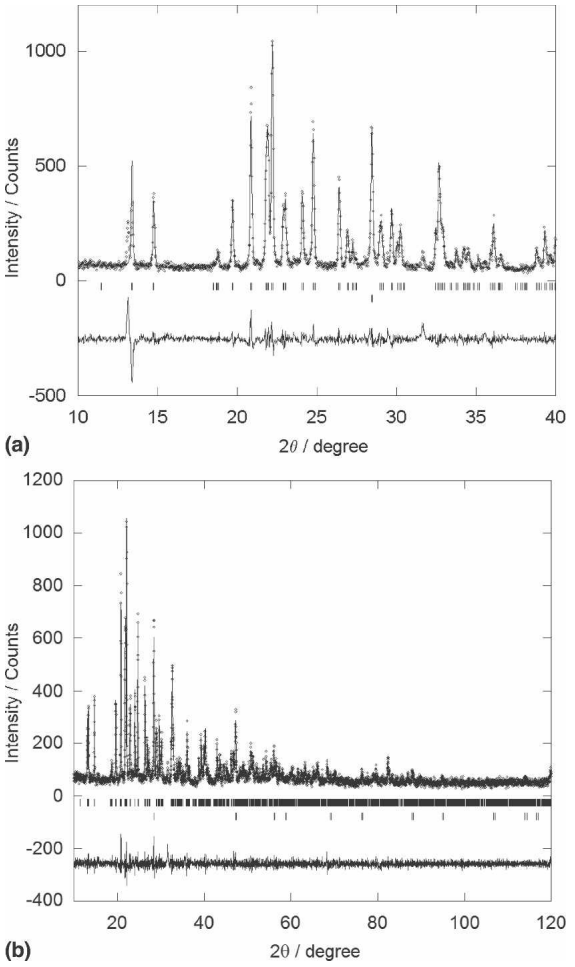

FIG. 2. Le Bail fits of the 473 K XRD data for $MgHf(WO_4)_3$ in (a) space group *Pnca* and (b) space group *Pnma*. Diamonds represent data points; the calculated pattern corresponds to the solid line, and a difference plot is shown below the pattern. Tick marks indicate peak positions for $MgHf(WO_4)_3$ (top) and the Si standard (bottom).

expansion along *a* and *c*. The relative expansion coefficients for the orthorhombic phase in the 400 to 800 K temperature range are $\alpha_a = -5.2 \times 10^{-6}$ K^{-1}, $\alpha_b = 4.4 \times 10^{-6}$ K^{-1}, $\alpha_c = -2.9 \times 10^{-6}$ K^{-1}, $\alpha_V = -3.7 \times 10^{-6}$ K^{-1}, and $\alpha_l = -1.2 \times 10^{-6}$ K^{-1}, respectively. No abrupt change in unit-cell volume was observed at the transition temperature, suggesting a second-order phase transition. This behavior is very different from that observed for other $A_2(MO_4)_3$ materials, which undergo a first order monoclinic ($P2_1/a$) to orthorhombic (*Pnca*) phase transition associated with a significant increase in unit-cell volume. This difference could be related to the fact that the orthorhombic structures are not identical.

IV. CONCLUSIONS

$MgHf(WO_4)_3$ undergoes a reversible phase transition from monoclinic to orthorhombic symmetry between 400 and 473 K. Monoclinic $MgHf(WO_4)_3$ was observed for the first time for temperatures up to 400 K. It adopts the same monoclinic structure as other $A_2(MO_4)_3$ compounds in space group $P2_1/a$ with an ordered arrangement of the +2/+4 cations, but it transforms to a different

TABLE I. Refinement results for variable-temperature powder x-ray and neutron diffraction data of $MgHf(WO_4)_3$. Monoclinic volume is divided by 2 to scale to orthorhombic results.

Temperature (K)	*a* (Å)	*b* (Å)	*c* (Å)	β (°)	Volume (Å^3)
X-ray diffraction data					
298	16.297	9.606	19.038	125.639	1209.639
373	16.298	9.603	19.029	125.670	1209.716
473	9.594	13.253	9.511	90.000	1209.394
573	9.586	13.261	9.509	90.000	1208.858
673	9.582	13.267	9.506	90.000	1208.296
773	9.578	13.273	9.503	90.000	1208.066
873	9.577	13.275	9.502	90.000	1208.011
Neutron diffraction data					
4	16.297	9.603	19.029	125.668	1209.679
200	16.297	9.603	19.029	125.669	1209.693
400	16.298	9.603	19.028	125.669	1209.677
550	9.586	13.261	9.509	90.000	1208.887
700	9.582	13.266	9.506	90.000	1208.307

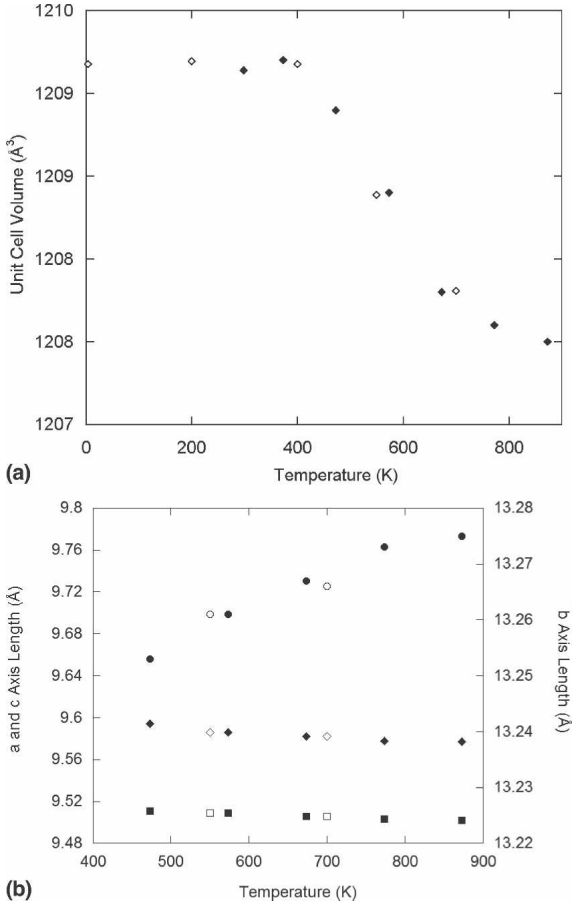

FIG. 3. Expansion of $MgHf(WO_4)_3$ from neutron (open symbols) and XRD (filled symbols) data. (a) Volume expansion. (b) Linear expansion coefficients in the orthorhombic phase along *a* (diamonds), *b* (squares), and *c* (circles) axes.

orthorhombic space group, *Pnma*. The reversibility of the phase transition suggests that the atomic connectivity in *Pnma* must be similar to that of the *Pnca* and $P2_1/a$ polymorphs. However, these subtle differences result in distinct properties of the two phases at the phase transition temperature: The $P2_1/a$ to *Pnca* conversion is a first-order transition associated with a sharp increase in unit cell volume, whereas second-order behavior is observed for $MgHf(WO_4)_3$ during the $P2_1/a$ to *Pnma* transformation. Second-order behavior offers advantages for potential applications of NTE materials in composites, where a sudden change in cell volume during a first-order transition can lead to composite deterioration through cracking. $MgHf(WO_4)_3$ shows negative-volume thermal expansion in the orthorhombic phase up to its decomposition above 873 K.

ACKNOWLEDGMENTS

This research was funded by the National Science Foundation under Grant DMR-0545517. We acknowledge the support of the National Institute of Standards and Technology, United States Department of Commerce, in providing the neutron research facilities used in this work. The authors would like to thank J. Stalick and J. Leao for their help with the experiments.

REFERENCES

1. V. Korthuis, N. Khosrovani, A.W. Sleight, N. Roberts, R. Dupree, and W.W. Warren: Negative thermal-expansion and phase-transitions in the $ZrV_{2-x}P_xO_7$ series. *Chem. Mater.* **7,** 412 (1995).
2. T.A. Mary, J.S.O. Evans, T. Vogt, and A.W. Sleight: Negative thermal expansion from 0.3 to 1050 kelvin in ZrW_2O_8. *Science* **272,** 90 (1996).
3. A.W. Sleight: Negative thermal expansion materials. *Curr. Opin. Solid State Mater. Sci.* **3,** 128 (1998).
4. A.W. Sleight: Isotropic negative thermal expansion. *Annu. Rev. Mater. Sci.* **28,** 29 (1998).
5. G. Ernst, C. Broholm, G.R. Kowach, and A.P. Ramirez: Phonon density of states and negative thermal expansion in ZrW_2O_8. *Nature* **396,** 147 (1998).
6. J.S.O. Evans: Negative thermal expansion materials. *J. Chem. Soc., Dalton Trans.* 3317 (1999).
7. T.A. Mary and A.W. Sleight: Bulk thermal expansion for tungstate and molybdates of the type $A_2M_3O_{12}$. *J. Mater. Res.* **14,** 912 (1999).
8. R. Mittal, S.L. Chaplot, H. Schober, and T.A. Mary: Origin of negative thermal expansion in cubic ZrW_2O_8 revealed by high pressure inelastic neutron scattering. *Phys. Rev. Lett.* **86,** 4692 (2001).
9. P.M. Forster and A.W. Sleight: Negative thermal expansion in $Y_2W_3O_{12}$. *Int. J. Inorg. Mater.* **1,** 123 (1999).
10. P.M. Forster, A. Yokochi, and A.W. Sleight: Enhanced negative thermal expansion in $Lu_2W_3O_{12}$. *J. Solid State Chem.* **140,** 157 (1998).
11. J.S.O. Evans, T.A. Mary, and A.W. Sleight: Negative thermal expansion in a large molybdate and tungstate family. *J. Solid State Chem.* **133,** 580 (1997).
12. T. Suzuki and O. Atsushi: Negative thermal expansion in $(HfMg)(WO_4)_3$. *J. Amer. Ceram. Soc.* **87,** 1365 (2004).
13. J. Rodriguez-Carvajal: Recent advances in magnetic structure determination by neutron powder diffraction. *Phys. B: Condens. Matter* **192,** 55 (1993).
14. W.M. Yim and R.J. Paff: Thermal expansion of AlN, sapphire, and silicon. *J. Appl. Phys.* **45,** 1456 (1974).
15. R. Shirley: *The Crysfire 2002 System for Automatic Powder Indexing: User's Manual* (The Lattice Press, Guildford, 2002).
16. J.W. Visser: A fully automatic program for finding the unit cell from powder data. *J. Appl. Crystallogr.* **2,** 89 (1969).
17. A. Boultif and D. Louër: Indexing of powder diffraction patterns for low-symmetry lattices by the successive dichotomy method. *J. Appl. Crystallogr.* **24,** 987 (1991).
18. P-E. Werner, L. Eriksson, and M. Westdahl: TREOR, a semi-exhaustive trial-and-error powder indexing program for all symmetries. *J. Appl. Crystallogr.* **18,** 367 (1985).
19. D. Taupin: A powder-diagram automatic-indexing routine. *J. Appl. Crystallogr.* **6,** 380 (1973).
20. F. Kohlbeck and E.M. Hörl: Indexing program for powder patterns especially suitable for triclinic, monoclinic and orthorhombic lattices. *J. Appl. Crystallogr.* **9,** 28 (1976).